Junctional Membrane Uncoupling

Permeability transformations at a cell membrane junction

W. R. LOEWENSTEIN, M. NAKAS, and S. J. SOCOLAR

From the Cell Physics Laboratory, Department of Physiology, College of Physicians and Surgeons, Columbia University, New York 10032

ABSTRACT The permeability of the membrane surfaces where cells are in contact (junctional membranes) in *Chironomus* salivary glands depends on Ca^{++} and Mg^{++}. When the concentration of these ions at the junctional membranes is raised sufficiently, these normally highly permeable membranes seal off; their permeability falls one to three orders, as they approach the nonjunctional membranes in conductance. This permeability transformation is achieved in three ways: (*a*) by iontophoresis of Ca^{++} into the cell; (*b*) by entry of Ca^{++} and/or Mg^{++} from the extracellular fluid into the cell through leaks in the cell surface membrane (e.g., injury); or (*c*) by entry of these ions through leaks arising, probably primarily in the perijunctional insulation, due to trypsin digestion, anisotonicity, alkalinity, or chelation. Ca^{++} and Mg^{++} appear to have three roles in the junctional coupling processes: (*a*) in the permeability of the junctional membranes; (*b*) in the permeability of the perijunctional insulation; and (*c*) a role long known—in the mechanical stability of the cell junction. The two latter roles may well be closely interdependent, but the first is clearly independent of the others.

INTRODUCTION

A wide variety of epithelial tissues are now known in which cells are in close communication. At the junctions of these cells, surface membrane permeability is so modified that many kinds of ions and molecules can move freely from one interior to another (Loewenstein and Kanno, 1964; Loewenstein et al., 1965; Potter et al., 1966; Loewenstein, 1966). This paper deals with the question of the stability of cell communication. The question is obviously linked with that of structural (mechanical) stability of the junctional elements which hold the cells together, and our first steps in exploring the question were guided by procedures long in use for mechanical dissociation of cells: Ca^{++} removal, trypsin digestion, and application of solutions of high pH (Ringer, 1890; Herbst, 1900; Roux and Jones, 1916; Chambers, 1940; Holtfreter,

1948; Moscona, 1952; Rinaldini, 1958). As it turned out, these procedures could be used in much milder forms than those required for mechanical cell separation. All of them caused interruption of communication (hereafter referred to as *uncoupling*) without noticeable changes in cell adhesion. All these procedures are known also to increase to some extent permeability of nonjunctional membranes (e.g., skeletal muscle cells). It was, therefore, clear from the outset that uncoupling can be demonstrated only if the junctional effects develop before the nonjunctional membranes become too leaky. In fact, with some procedures the nonjunctional effects turned out to be sufficiently slow or small enough to allow analysis of some of the factors involved in maintaining junctional communication.

For the present study we chose the salivary gland cells of the midge *Chironomus thummi*, which have junctions of the septate type. These cells offer a number of advantages. In the stage studied, they are arranged in a single chain (there are typically 20–30 cells in a gland); they are large (100–200 μ

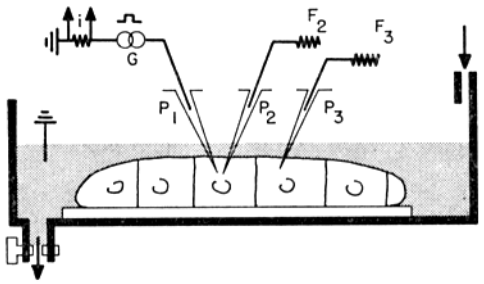

FIGURE 1. Diagram of setup. Description in the text.

in diameter); and the resistive properties of their surface membranes remain stable throughout the duration of the experiments (½–2 hr).

Cell communication was measured with an electrical technique described in an earlier paper (Loewenstein and Kanno, 1964). It consists essentially of injecting a current of ions into a cell of the chain and then determining what fraction of the current leaks to the cell exterior across the nonjunctional membranes of this cell, and what fraction leaks into the adjacent cell across the junctional membranes.

Brief accounts of some of the results have already appeared (Nakas et al., 1966; Socolar et al., 1967).

METHODS

Preparation Salivary glands of fourth instar larvae of *Chironomus thummi* were used. At this developmental stage, the electrical coupling between the cells is at its maximum (Loewenstein et al., 1965), and the cell membranes' resistive properties are most stable. The glands were isolated and mounted in a glass chamber (Fig. 1). A wisp of glass, drawn out of a capillary, immobilized the gland against the bottom of the chamber.

Electrical Arrangement Three glass micropipettes filled with 3 M KCl were inserted into two contiguous gland cells (Fig. 1). One pipette (P_1) served to pass rectangular pulses of current (usually outward) of 100–120 msec duration, delivered by a constant-current device (G) coupled electrooptically to the pipette (Baird, 1967), and the other two (P_2, P_3), to record the resulting voltage drops. The voltages from the pipettes were fed into DC amplifiers through field effect transistor input stages (F_2, F_3); the voltages were displayed either alternately by means of a switching device on one beam, or simultaneously, on two beams of an oscilloscope. With the currents used, potentials of the cell exterior, both basal and luminal, were usually within 0.2 mv of ground (and never beyond 2 mv). Current was displayed (i) simultaneously with the voltage on the second or third trace of the oscilloscope. This arrangement provided measures of junctional cell communication and cell surface membrane impedance. It provided at the same time an index of the state of the cells: in measuring the (input) impedance across the surface of the cell system, it offered a sensitive indicator of membrane injury or imperfections in membrane sealing around the micropipettes. Normal cell resting potentials were inside-negative and averaged 23 ± 6 mv standard deviation (24 cases). During the course of treatment with uncoupling agents, the resting potential usually declined, typically by 60 to 80%.

The micropipettes had tip diameters below 0.2 μ and resistances of 10–20 meg Ω (P_1) and 15–30 meg Ω(P_2 and P_3). They were driven by micromanipulators equipped with a vibration-free hydraulic advance mechanism operating in the direction of pipette axis. Pipette insertion and all related manipulations were done under a stereomicroscope.

The micropipettes were kept inside the cells for the duration of the experiments. Experiments lasted from 30 min to 2 hr. Good preparations could be maintained for 2 hr without changes in the conductive properties of the membranes. In this respect, *Chironomus* salivary glands offered a clear advantage over other epithelial cells, such as *Chironomus* renal, *Drosophila* salivary gland, and toad urinary bladder cells, which we tested in preliminary runs in search of a suitable cell material.

Membrane Perforation For the drilling of holes into the surface membrane in the experiments of the kind illustrated in Fig. 13, relatively blunt micropipettes (0.5–1 μ diameter) were moved repeatedly in and out of the cells. In successful runs this could be done without dislodging the intracellular microelectrodes. For coarse cuts into the cell surfaces in the experiments of the kind illustrated in Fig. 14, sharp steel needles were used. These cuts were made before insertion of the microelectrodes.

Ca Injection Ca was injected into the cells with micropipettes (of the same type as those used for electrical measurements) filled with a solution 0.1 M in both $CaCl_2$ and KCl. With this combination, the pipettes had tolerable resistances (25–35 meg Ω:), and their tips were not clogged in cytoplasm. Ca ions were driven into the cells with rectangular current pulses of 5×10^{-10} to 1×10^{-9} amp and 40 msec duration at a rate of 5 pulses/sec (Fig. 9, inset). The amount of Ca^{++} injected (m_{Ca}) was estimated from:

$$m_{Ca} = \frac{nIt}{2F} \qquad (1)$$

where I is the current; t, total duration of injection current; F, Faraday's constant; and n, the transference number, taken to be 0.4. (Only a rough estimate is possible here. The current is assumed to be carried by the K^+ and Ca^{++} of the micropipette and by the intracellular anions, assumed to be divalent and at a concentration of 0.1 M. All these ions are taken to have comparable mobilities.) The total Ca concentration was calculated on the basis of an average cell volume of 5×10^{-7} cc.

Media

CHELATORS

1. Disodium ethylenediaminetetraacetate (EDTA; Fisher Scientific Co., Springfield, N.J.).

2. Ethylene glycol-bis(β-aminoethyl ether)-N,N'-tetraacetic acid (EGTA; Eastman 8276, Distillation Products Industries, Rochester, N.Y.); this was titrated to pH 6.3 with NaOH.

SOLUTIONS

1. *Normal saline:* 87 mM NaCl; 2.7 mM KCl; 1.3 mM $CaCl_2$; 10 mM Tris buffer; pH 6.3.

2. *Solutions with reduced or enriched Ca:* $CaCl_2$ of the normal saline exchanged with NaCl on an equimolar basis.

3. *Chelator solutions:* normal saline with EDTA-$CaCl_2$, EGTA-$CaCl_2$, or EGTA-$MgCl_2$ mixtures, or just EGTA, substituted for NaCl on an equimolar basis.

4. *Hypertonic solutions:* normal saline + sucrose to give total osmolarities varying between one and two times normal.

5. *Hypotonic solutions:* normal saline reduced in NaCl to give total osmolarities ranging between 1 and 0.5 times normal.

6. *Solutions with high pH:* Disodium phosphate was used instead of Tris buffer of normal saline. With total phosphate sufficiently low, it is possible to keep the free $[Ca^{++}]$ constant over the entire range of pH variation (pH 7–10) (La Mer, 1962). For example, 2.8×10^{-6} M phosphate, though providing little buffering capacity, sufficed to keep the medium within 0.3 pH unit of pH 10, as checked after the experiments.

7. *Trypsin* (salt-free, crystallized, Mann Research Laboratories, New York, N.Y.) 10,000 BAEE units/mg, 0.01–0.1 % in normal saline.

The solution referred to as control saline in the experiments with chelators (Figs. 2, 9, 11, and 13) was normal saline, calcium-free. Although the membrane resistance, both junctional and nonjunctional, turned out to be not noticeably different in normal and Ca-free salines (see, for example, Fig. 4), a Ca^{++}-free saline seemed to us a more appropriate control for the experiments in which $[Ca^{++}]$ was to be varied.

The osmolarity of solutions 1, 2, 6, and 7 was uniform within 1 %; the osmolarity of solutions 3 deviated at most by +4% except in the case of Fig. 2 A, where it deviated by +9%. The pH of solutions 1, 2, 3, 4, 5, and 7 was 6.3.

The concentrations of free divalent cations in the chelating media were calculated, for the appropriate pH, from the chelator acid dissociation constants and metal-complex dissociation constants (Chabereck and Martell, 1959).

RESULTS

Uncoupling by Chelators

JUNCTIONAL AND NONJUNCTIONAL PERMEABILITY CHANGES Fig. 2 illustrates two experiments in which application of a saline containing a chelator

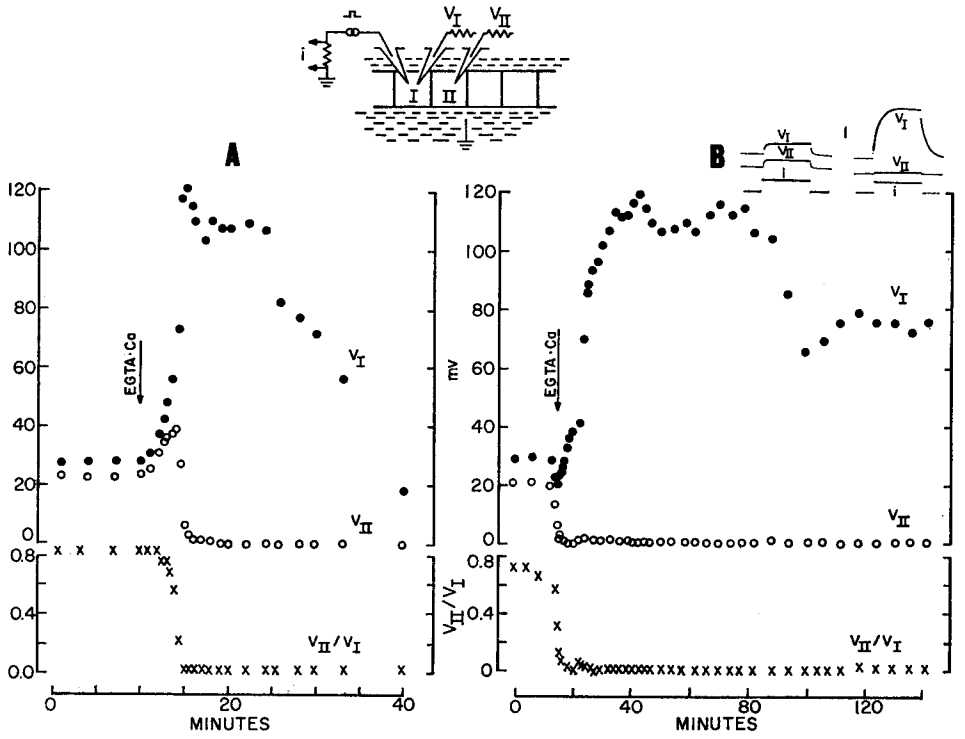

FIGURE 2. Junctional uncoupling by chelator action. Current pulses are passed between the inside of cell *I* and cell exterior, and the resulting membrane voltages (V) are recorded in cells *I* and *II*, as diagrammed in the top inset. Upper ordinates, membrane voltages V_I and V_{II}. Lower ordinates, V_{II}/V_I. (A) At arrow, control saline is replaced by solution containing 10.0 mM Ca and 20.4 mM EGTA (free $[Ca^{++}] = 5 \times 10^{-6}$ M). (B) At arrow, the control saline bathing the preparation is replaced by a solution with 1.00 mM EGTA and 1.49 mM Ca (free $[Ca^{++}] = 0.5$ mM). Inset, samples of oscilloscope recording of V and i before (left) and after (right) uncoupling. Calibration, 20 mv; current pulse duration, 120 msec. (Current in this and subsequent figures, unless stated otherwise, 5×10^{-8} amp.)

(EGTA) to the salivary gland causes complete uncoupling of the gland cells. A constant current generator passed current pulses from the inside of a cell (*I*) to the exterior, and the resulting membrane voltages were recorded in this cell and in a contiguous one (*II*). The ratio of the membrane voltages, V_{II}/V_I (*coupling ratio*), provides a convenient index of cell communication. Within 5 min of the application of the solution, virtually all intercellular communica-

tion was cut off; the coupling ratio fell toward zero: V_{II} decreased by at least an order of magnitude, while V_I increased severalfold. This fall in coupling ratio or, in fact, any diminution in coupling ratio, will, as a matter of operational definition, be termed uncoupling.

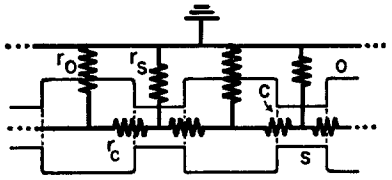

FIGURE 3. Scheme and equivalent circuit of the cell chain. *C*, junctional membranes; *O*, nonjunctional surface membranes of cells; *S*, perijunctional insulation.

TABLE I

RESISTANCE CHANGES IN JUNCTIONAL UNCOUPLING BY CHELATORS IN PRESENCE OF Ca ION*

Experiment No. ‡	V_I		V_{II}		r		r_j		r_e	
	Normal	Uncoupled	Normal	Uncoupled	Normal	Uncoupled	Normal	Uncoupled	Normal	Uncoupled
	mv	*mv*	*mv*	*mv*	*MΩ*	*MΩ*	*MΩ*	*MΩ*	*MΩ*	*MΩ*
2 D	18.5		14.5		0.9–3		0.09–0.18		0.04–0.09	
		51.0		5.7		1.3		9		1.6–4
14 G	43.0		35.0		1.1–4		0.09–0.18		0.04–0.09	
		131.5		4.0		1.4		43		2.5–22
20 G	15.0		10.0		0.5–1.5		0.12–0.24		0.06–0.12	
		53.4		2.5		1.2		23		1.9–11
X 2 D	19.8		18.5		1.8–10		0.03–0.09		0.01–0.04	
		126.3		3.5		2.7		91		4.8–46
X 3 D	23.5		20.5		1.5–7		0.06–0.15		0.03–0.07	
		66.5		5.0		1.6		18		2.3–9
X 8 G§	28.5		23.4		1.5–6		0.11–0.23		0.06–0.11	
		119		6.0		2.6		47		4.3–24
X 11 G‖	40.0		34.5		2.4–10		0.12–0.26		0.06–0.13	
		115		3.0		2.4		88		4.8–44

* "Normal" values are those prevailing before chelator is applied; "uncoupled," at or about time that V_I reaches its maximum. In all cases, free $[Ca^{++}]$ was $\geq 10^{-5}$ M and $\leq 5 \times 10^{-4}$ M. Current 5×10^{-8} amp in all cases except No. 14 G, where it was 10^{-7} amp.

‡ Suffix "D" indicates chelator was EDTA; "G" indicates EGTA.

§ Same experiment as Fig. 2 A.

‖ Same experiment as Fig. 10.

It is useful to consider the above results in terms of the electrical equivalent of the connected cell system (Fig. 3; since only steady states of current will be considered, the conductive but not the reactive elements are shown). A fall in V_{II} (Fig. 2 A) might result from either a rise in junctional membrane resistance r_c, a fall in perijunctional insulation resistance r_s, or a fall in nonjunctional surface membrane resistance r_o. But since the fall in V_{II} is accompanied

by a rise in V_I, the last alternative is inadequate; it is necessary to have either (*a*) a rise in r_c, or (*b*) a fall in r_s together with a rise in r_o.

In fact, a large increase in r_c does occur. An approximate computation (Appendix) from the data of Fig. 2 A shows that r_c increased at least 40-fold, and perhaps as much as 400 times, upon uncoupling (in particular, by the time V_I attained its peak). *This means that the formerly closely communicating cells have sealed themselves off. Generally the ion permeability of the junctional membrane in such measurements fell by one to three orders of magnitude* (see r_c, Table I). (In the normally coupled cell system, the value of r_c here, as in other epithelia, is of an order attributable to the cytoplasm alone (Loewenstein et al., 1965).)

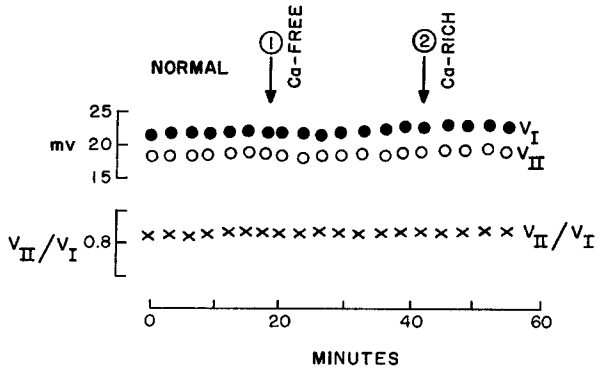

FIGURE 4. Insensitivity of the cell system surface to extracellular Ca^{++}. The normal saline bathing the preparation is replaced by Ca^{++}-free saline (arrow 1), and saline containing three times normal Ca^{++} concentration (arrow 2). V_{II}/V_I axis range 0.6-1.0.

In contrast to r_c, r_o appears to change little in magnitude, although it cannot be estimated as directly (see Appendix). A priori, a rise in r_o is unlikely: generally the resistance of cell surface membranes, if it changes at all in response to Ca depletion, falls. In the present preparation, the nonjunctional resistances are insensitive to variation of external [Ca^{++}] over a considerable range (Fig. 4). In the absence of independent information about r_s, no upper limit for r_o can be inferred from the experimental data. But a reasonable upper limit in the normally coupled state is obtained by taking the specific resistance of the *O* element (Fig. 3) as 10^4 Ω cm², the highest normally encountered in various kinds of cell membranes, and the area of *O* as 10^{-3} cm², an area obtained from electron micrographs. This gives 10 M Ω as the upper limit for r_o in the normally coupled state. For the experiment of Fig. 2 A, the lower limit for r_o is 2.6 M Ω after uncoupling, at the time of peak V_I. Thus it is unlikely that r_o has changed by more than a fourfold diminution during the much larger increase of r_c. More generally, in experiments of this kind, the same reasoning indicates that r_o probably falls at most by one order of mag-

nitude. This can be seen from Table I, where the lower limit for r_o in the uncoupled state is given for seven cases by the values under the heading r.

As to changes in r_s, the present results provide no clue. There is reason to expect that r_s might fall during uncoupling: chelators, as well as the other uncoupling agents used in the present work, can lead to cell separation if their action is intense and sustained.

Another feature of Fig. 2 A is the short lived rise of V_{II} when the chelator is introduced. Such a rise, although absent in a majority of our experiments, nevertheless occurs frequently. Its occurrence is readily understood in terms of the cable representation of the cell chain. In this representation, the potential across the outer membrane, at any distance x from the current electrode, is proportional to the input resistance and to an attenuation factor exp $(-x/\lambda)$, where λ is the "length constant." If $x \ll \lambda$, as is the case for V_{II} in the normally coupled state, a small initial rise in r_c gives rise to a larger input resistance; and this predominates initially over the increased attenuation due to the simultaneous fall of the length constant. But as λ becomes smaller, eventually the declining attenuation factor assumes dominance over the rising input resistance, so that further increase of r_c leads to fall of V_{II}. Thus an early, short lived rise of V_{II} would appear to be a general expectation. Two possible explanations for its frequent failure to appear suggest themselves. (*a*) The early dominance of rising input resistance over falling length constant is absent if the early rise of r_c is accompanied by sufficient diminution of r_o. (*b*) In some preparations the normally coupled cell chain in which measurements were made may have constituted only a small part of the entire cell chain; possible injuries may have led to the uncoupling of major portions of the chain. The foregoing prediction of a rise in V_{II} does not apply to a very short chain, e.g., three cells.

In a number of cases (e.g., Fig. 2 B), V_I remained near its peak value, or (post-peak) at a lower finite value, for an extended time, even for 30 min. This stabilization would appear to mean that r_o was (or had become) constant and that r_c had become so large that each cell was isolated from its neighbors, thus making V_I rather insensitive to changes in r_s, if any. In no case, however, could uncoupling be halted or reversed by a return to normal or Ca-rich saline (up to four times normal [Ca^{++}]); this was so regardless of the stage of uncoupling. (Time for exchange of solutions was 20–30 sec.)

Uncoupling by Alkalinity

Junctional communication is impaired if the extracellular fluid is made sufficiently alkaline. Fig. 5 shows an example in which the pH of the bathing saline is varied from 7 to 10. At pH 10 the cell system uncouples and, as in the case of uncoupling by chelators, this is associated with sealing of the junctional membranes: the coupling ratio falls to zero and V_I rises steeply. Computation of the resistances shows that by the time V_I attains its peak, r_c has risen from an initial value in the range of 0.01–0.05 M Ω to 3–6 M Ω.

In this particular example V_I falls 5 min after the first signs of uncoupling.

In some demonstrations of uncoupling in alkaline media, V_I remained near its peak level as long as 30 min.

Uncoupling at high pH may be reversible to some degree. This is suggested by the experiment of Fig. 5 in which return to pH 7 causes current to flow again into cell *II*; V_{II} rises again from level zero, the coupling ratio reaching almost the original value of the normally coupled system. Subsequent shift to pH 10 produces new uncoupling with signs of new junctional sealing. We were able to show recoupling in only one case (Fig. 5). The single result provides, of course, not more than a suggestion of reversibility.

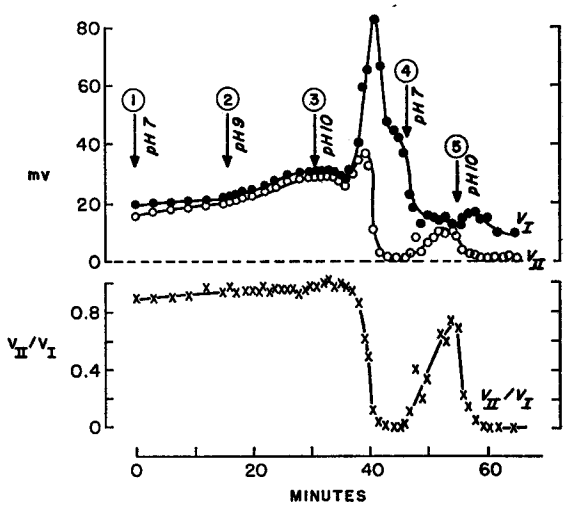

FIGURE 5. Uncoupling at high pH. Arrows denote application of salines and their pH. Ca^{++} concentration is constant at 1.29 mM in all salines.

Uncoupling by Trypsin Action

Application of trypsin leads to fast uncoupling. Fig. 6 shows the effects of a 0.05% solution of trypsin in saline (7×10^{-6} M). Within less than 1 min of enzyme application, the first signs of junctional sealing appear; and within 2–4 min all junctional coupling seems lost. Uncoupling could not be reversed by washing the preparation in trypsin-free saline. The value of r_e rose from the normal 0.07–0.14 M Ω, reaching 0.3–0.9 M Ω at the peak of V_I.[1]

Uncoupling by Changes in Tonicity

In the following experiments, we tried to produce uncoupling by the action of mechanical forces. In one series of experiments this was attempted by pulling

[1] The V_I rise seen in Fig. 6 is sometimes absent even when computation shows an r_e rise comparable to the one here. In such cases, there occurs a more pronounced drop in the value of the parameter r of the reduced equivalent network (see Appendix).

cells apart with the aid of micromanipulated glass instruments. These attempts failed. They all led to rupture of the surface membranes.

We were more successful in another series of experiments in which the tonicity of the extracellular fluid was changed. Uncoupling with junctional sealing occurred in hypertonic media (Fig. 7), but has not been attainable in hypotonic conditions. The uncoupling here may have been due to unbalancing of tensile forces at the cell junction during changes of tonicity, or to increase in permeability at the nonjunctional cell membrane (see below).

Uncoupling could be demonstrated by sucrose additions giving osmolarity 1.5–2 times control level. With these, uncoupling starts within 1 min of the tonicity changes and the alterations in r are sufficiently slow to disclose

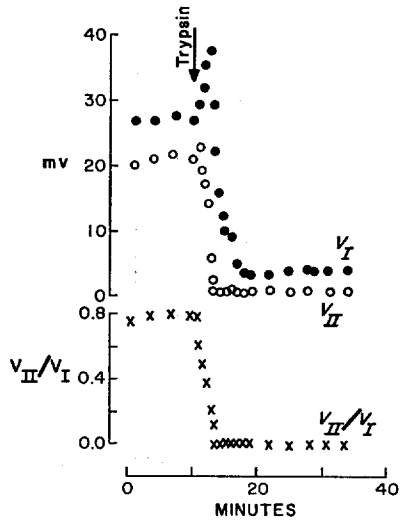

FIGURE 6. Uncoupling by trypsin. At arrow, normal saline is replaced by one containing 0.5 mg/ml of trypsin.

junctional sealing in the form of a rise of V_I to a peak value several times normal, as in the case of uncoupling by chelators. In the experiment of Fig. 7, r_c rose from 0.06–0.12 M Ω in the normally coupled state to a value in the range 1.5–5 M Ω upon uncoupling (when V_I was 94.5 mv, 2 min after its peak). Meanwhile r declined from 1.25–2.7 to 1.15 M Ω.

Some General Aspects of Uncoupling

Several features were common to uncoupling whatever the agent used except for trypsin. So long as the free [Ca^{++}] in the bath was at least about 10^{-5} M, the resistance (r_c) of the junctional membrane rose by at least one, and perhaps two or three orders of magnitude by the time V_{II} became too small for computations, and r_c was still rising even then. (From the action of trypsin, only a two- to twentyfold rise in r_c resulted.) On the other hand, by the same kind of inference made in the chelator experiments, it appears that with the

other agents, too, r_o changed at most by one order in the time interval of the r_c rise. In many cases, V_I stabilized at a substantial value after uncoupling, suggesting a rather mild action by the uncoupling agents on r_o.

The Roles of Divalent Cations in Junctional Uncoupling and Sealing

CONDITIONS FOR JUNCTIONAL SEALING It is evident that the junctional membranes (r_c), highly permeable in the normally connected cells, become relatively impermeable in the course of uncoupling. This sealing process

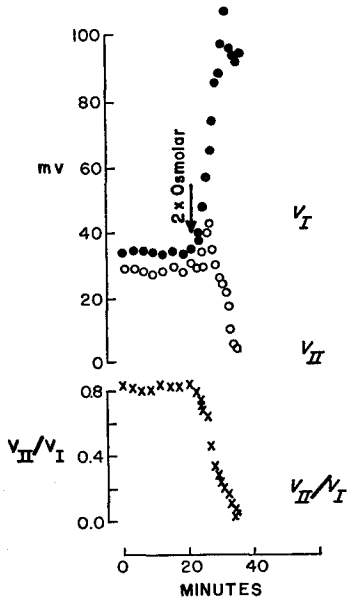

FIGURE 7. Uncoupling by hypertonic solution (current, 1×10^{-7} amp). At arrow, normal saline replaced by saline twice osmolar.

invariably ensues when uncoupling occurs in media of normal ionic concentrations. Aside from its functional relevance to problems in cellular communication, this phenomenon is of interest purely in terms of membrane behavior.

The sealing process was first noticed in experiments on uncoupling by chelators. It was then observed that the process occurred when the concentration of free extracellular Ca^{++} was between 10^{-3} and 10^{-5} M, and only then. This puzzling situation resolved itself when the later results of uncoupling by trypsin, anisotonic, and alkaline actions all showed that the sealing process occurred whenever the concentration of extracellular free Ca^{++} was greater than about 10^{-5} M.[2] It became clear then that the above-mentioned limits of 10^{-3} M and 10^{-5} M reflected the limits of two entirely different processes: the

[2] It is technically difficult to obtain precise threshold values of Ca^{++} concentration for junctional sealing. The minimum free [Ca^{++}] required for sealing was between 10^{-5} and 10^{-4} M in the various trials.

former is the upper limit of Ca^{++} concentration that allows opening of leaks for Ca^{++} through a cellular surface barrier (see Discussion), while the latter is the lower limit for the sealing of the junctional membranes.

The experimental demonstration of these propositions for the case of uncoupling by chelator is illustrated in Fig. 8. At concentrations of free Ca^{++} of 10^{-5} M or lower in the bathing fluid, the ratio V_{II}/V_I falls without rise in V_I; uncoupling seems to occur without junctional membrane sealing. Subsequent addition of Ca^{++}, increasing the free Ca^{++} concentration to 10^{-4} M, caused

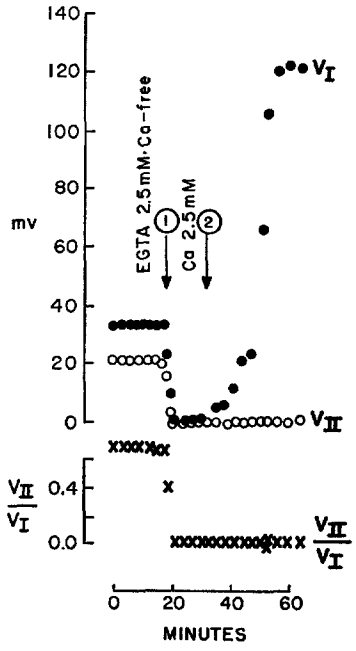

FIGURE 8. The sealing action of Ca. Arrow 1, control saline replaced by Ca-free chelator saline containing 2.5 mM EGTA. Arrow 2, addition of 2.5 mM Ca^{++} to the chelator saline; free $[Ca^{++}]$ = 0.1 mM. Current, 1×10^{-7} amp.

sealing of the junctional communicating membranes that was reflected in the rise of V_I.

The sealing effect of Ca^{++} on the junctional communicating membranes is shown further by experiments of the kind illustrated in Fig. 9, in which Ca^{++} is driven into the cell by iontophoresis. The first injection (about 3×10^{-14} mole) of Ca^{++} near the junctional membranes sufficed to raise the mean Ca concentration inside a single cell by about 10^{-4} M. It caused a rise in V_I, reaching a peak 10 min after injection (Ca^{++} applications to the nonjunctional membrane surfaces via the bathing medium produce no appreciable change in either junctional or nonjunctional resistance, Fig. 4).

The reduction of junctional permeability by action of Ca^{++} has recently been shown also in electrical measurements on rat liver cell (Kanno and Loewenstein, unpublished; Loewenstein, 1966).

PARALLEL ACTION OF Ca^{++} AND Mg^{++} In all the foregoing experiments on uncoupling by chelators, the bathing medium lacked Mg^{++}. But uncoupling does not occur when there is a sufficiently high concentration of Mg^{++} in the extracellular fluid. Fig. 10 illustrates an example in which the preparation is bathed in a Ca-free saline containing an EGTA-$MgCl_2$ mixture having a free [Mg^{++}] of the order of 10^{-3} M (step 1); there is no detectable uncoupling. But subsequent application of chelator in a Mg^{++}-free solution (step 3) causes uncoupling despite the fact that the uncomplexed EGTA concentration is an

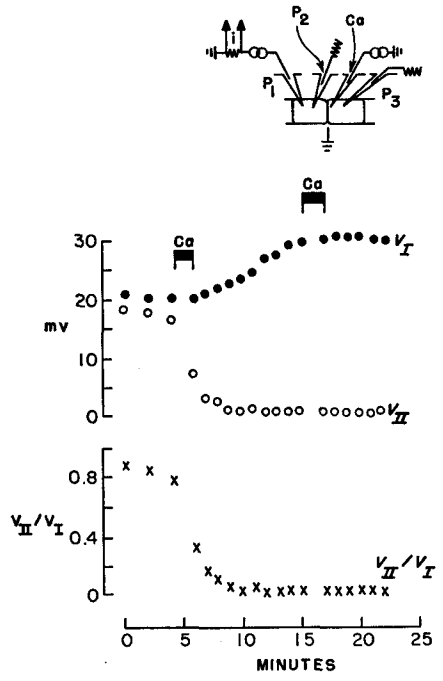

FIGURE 9. Changes in junctional communication due to intracellular injection of Ca^{++}. Ca^{++} ions are introduced into a cell by iontophoresis from a micropipette (*Ca*); the tip of the pipette lies near the junctional membrane. (The rest of the electrode arrangement is as in Fig. 1.) The black bars mark two periods of iontophoresis. A total of about 3×10^{-14} mole of Ca^{++} is injected in each period.

order of magnitude lower here than in step 1. Apparently Mg^{++} can substitute for Ca^{++} in maintaining junctional coupling.

The related question, whether Mg^{++} also substitutes for Ca^{++} in effecting junctional membrane sealing, was explored in a few experiments of the kind illustrated in Fig. 8 for Ca^{++}. The results were essentially like those in Fig. 8. Thus Ca^{++} and Mg^{++} appear to have parallel actions in this junctional phenomenon also. This has been shown recently in mammalian liver cells as well (Kanno and Loewenstein, unpublished; Loewenstein, 1966).

Chelation As a Mechanism of Uncoupling Four possible modes of action by chelators suggest themselves here. The chelator molecule may detach a metal ion from a key cellular structure; it may detach an organic cation; it may bind to a cellular structure; or it may simply reduce the concentration of free

divalent cation. The first possibility seems the likeliest; (*a*) in media containing Ca^{++} and no Mg^{++}, uncoupling by chelators occurs whenever $[Ca^{++}]$ is below about 10^{-4} M; (*b*) normal coupling is maintained in 10^{-3} M free $[Mg^{++}]$ (e.g., Fig. 10) even in a concentration of uncomplexed EGTA two orders higher than that which suffices for uncoupling in much lower divalent cation concentrations;[3] (*c*) in tissues such as rat and mouse liver (Kanno and Loewenstein, unpublished; Loewenstein, 1966) and sponge cell aggregates (Loewenstein, 1967) uncoupling results upon mere omission of Ca^{++} and Mg^{++} from the

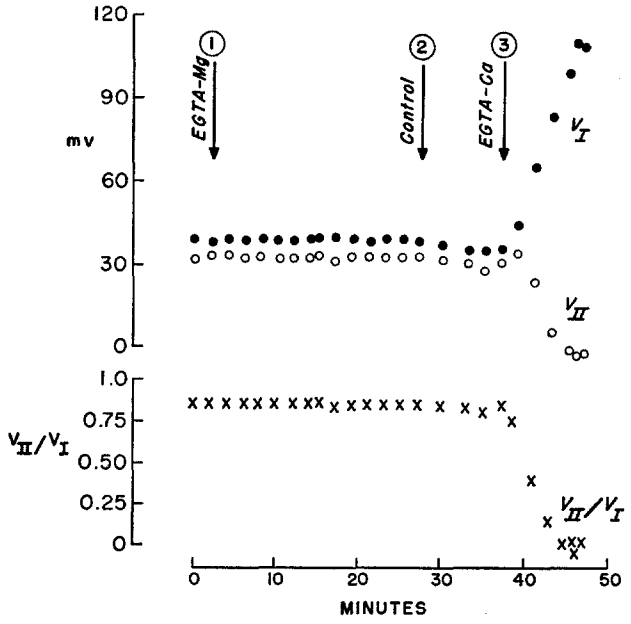

FIGURE 10. Uncoupling prevented in the presence of Mg^{++}. Arrow 1, control saline replaced by Ca^{++}-free saline with 2.5 mM EGTA, 2.5 mM $MgCl_2$ (free Mg^{++} in excess of 10^{-3} M). Arrow 2, back to control saline. Arrow 3, application of saline with 2.5 mM EGTA, 2.5 mM Ca (free $[Ca^{++}] = 1 \times 10^{-4}$ M).

bathing medium. The fact that the latter result has not been obtainable with the present preparation, in which chelators had to be used, suggests that divalent cations here are not so readily released to the bathing medium.

If the cation is represented as M^{++}, the binding anionic structural element in the tissue as X^{-}, and the chelator as $A^{=}$, the principal reaction in uncoupling in the present preparation may be representable as

$$MX_2 + A^{=} \rightleftarrows MA + 2X^{-}.$$

[3] The analogous experiment with Ca^{++} was not possible with available chelators. The stability constant of CaEGTA is six orders higher than that of MgEGTA. We know of no suitable chelator for which the reverse holds.

Presumably uncoupling occurs when the ratio $[A^-]/[MA]$ is made sufficiently high. Since we have, at the same time, the equilibrium

$$M^{++} + A^- \rightleftarrows MA,$$

this means that $1/[M^{++}] \propto [A^-]/[MA]$, and the concentration ratio condition for uncoupling appears to be simply a condition on $[M^{++}]$, so long as the identities of M^{++} and A^- are not varied. (At pH 6.3, the effective stability constants of CaEGTA and CaEDTA differ by one order of magnitude. This is about the limit of resolution in our data and hence the critical $[Ca^{++}]$ level for uncoupling would appear to be about the same for both chelators.) The greater the stability of the metal-tissue complex and the smaller the metal-chelate stability constant, the higher should be the concentration ratio required for uncoupling (see item (*b*) of the evidence cited in the preceding paragraph). Experiments are under way to test this explanation further.

As to the identity of the structural ion which normally maintains coupling, the most likely possibilities are, of course, Ca^{++} and Mg^{++}; they are the most abundant divalent cations in insect extracellular fluid. But nothing can be said yet about the relative importance of these ions.

DISCUSSION AND CONCLUSIONS

Intercellular Coupling

Intercellular communication emerges from the present results as a labile process. It is clearly much more labile than over-all intercellular adhesion. The physiological safety margins for communication, however, are still quite large. To produce alterations in communication one must push the cellular environment well beyond its normal physiological state (i.e., to pH > 9; tonicity well above control level; $[Ca^{++}]$ and $[Mg^{++}] < 10^{-3}$ M). In the course of this, a number of points are brought out which provide some insight into the physiology of cellular communication: (*a*) The cell, whose interior is functionally continuous with that of others in the normally connected cell system, becomes a unit in the sense of classical cell theory upon uncoupling; the normally highly permeable junctional membrane becomes relatively impermeable and is no longer so remarkably different from the nonjunctional surface in resistance. The basic structural matrix of the membrane must, therefore, have existed at all times at the junctional surfaces; only the permeabilities differed. (*b*) In the transformation of the junctional membranes from high to low permeability, divalent cations play a key role. The free Ca^{++} concentration on the cytoplasmic side of the junctional membranes is normally low ($<10^{-5}$ M; see for example Hodgkin and Keynes, 1957). In all likelihood this is also the case at the other sides, because the system is insulated from the extracellular fluid (Loewenstein and Kanno, 1964; Loewenstein et

al., 1965). At Ca^{++} concentrations above about 10^{-5} M, the transformation of membrane permeability takes place. (*c*) Intercellular communication does not result from mere apposition of cellular membranes. Once the membranes are uncoupled, cellular communication is not restored by mere proximity of the membranes. Probably a certain degree of structural organization is necessary to make a communicating junction. A high degree of organization appears, in fact, at the electron microscope level, where the septate junctions offer aspects of regular arrays in their over-all as well as in their subunit structure (Wiener et al., 1964; Locke, 1965; Bullivant and Loewenstein[4]).

To these points may be added a fourth, known from earlier results (Loewenstein and Kanno, 1964; Loewenstein et al., 1965): along its *entire* limiting surface, the normally connected cell system provides insulation of its interior from the extracellular medium.

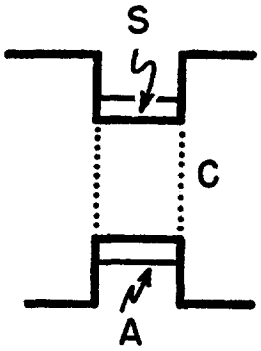

FIGURE 11. Junctional unit. Explanation in the text.

A picture of junctional processes that fits these points is described in detail elsewhere (Loewenstein, 1966). Here we shall discuss only the features immediately relevant to the present results. Fig. 11 gives the general picture. It is a functional diagram of a junctional unit including (*a*) the junctional membranes, *C*, and (*b*) the perijunctional resistive element *S* providing insulating surface continuity. To these has been added (*c*) a linking element *A* providing structural integrity. (*S* and *A* may, of course, be components of a single structure, or even identical structurally. The separation between the two *C* elements in the diagram is meant to indicate that they are separate structures, not necessarily the presence of an additional compartment.)

With respect to *C*, the hypothesis is made that certain divalent cation binding sites on it are normally unoccupied; with respect to *S*, that its integrity depends on that of *A*. No special assumption need be made for *A*; cell adhesion is known to depend on divalent cations and to be impaired by trypsin and

[4] Bullivant, S., and W. R. Loewenstein. Structure of coupled and uncoupled epithelial cell membrane junctions. Paper to be published.

alkalinity (Ringer, 1890; Herbst, 1900; Chambers, 1940; Holtfreter, 1948; Moscona, 1952).

In the light of this picture, the present results may be interpreted as follows. Permeability of the junctional membranes is normally high, primarily because these membranes are in an environment of low free [Ca^{++}] (and [Mg^{++}]?). Trypsin, chelators, OH^-, and anisotonicity make the surface insulation of the connected cell system permeable to divalent cations and hence expose the junctional membranes to the extracellular concentrations of these ions. If

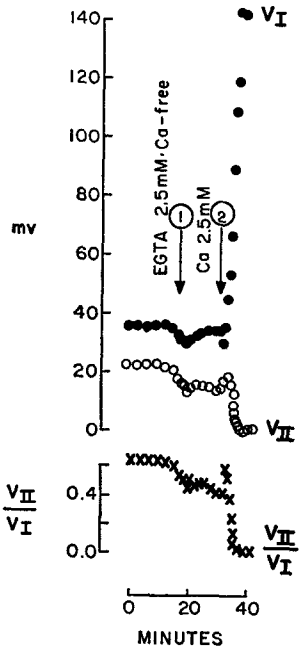

FIGURE 12. Minimal changes in surface insulation of the connected cell system during uncoupling by chelation. Arrow 1, control saline replaced by Ca-free chelator saline containing 2.5 mM EGTA. Arrow 2, addition of 2.5 mM Ca^{++} to the former saline; free [Ca^{++}] = 0.1 mM. Current, 1×10^{-7} amp.

these concentrations are sufficiently high, as they normally are, the junctional membranes become relatively impermeable.

A possible site at which the surface insulation becomes permeable to divalent cations is *S*. This is a good possibility because all procedures which have led to electrical uncoupling here will, if intensified, lead to mechanical uncoupling too; and, as is well known from tissue culture work, cells thus separated emerge each with complete and intact surface membrane equipment, and survive. The alternative is that *O* is the site of the initial change in permeability to divalent cations. This is not excluded by the present results.

Uncoupling can occur in fact with little change in surface resistance (see Table I and Appendix). A particularly striking instance is shown in Fig. 12, for the case of uncoupling by chelator action. Here EGTA causes quite small changes in V_I and V_{II} and, hence, in over-all surface insulation. Yet junctional

sealing occurs all the same when the extracellular [Ca^{++}] is made high enough. This pattern was rare in our experiments with chelators. But it may be singularly instructive: the common pattern is that of Fig. 8, and thus one might have been led to believe that electrical uncoupling follows only upon a rather gross leak in the insulating surface. In this connection it is interesting also that electron micrographs of junctions uncoupled electrically by mild chelation or hypertonicity, as in the present work, reveal no structural changes (Bullivant and Loewenstein[4]).

To sum up, *in the present view junctional uncoupling proceeds in two steps. First,* S *or* O *becomes a gateway for divalent cations. Then the junctional membranes* (C) *seal in the presence of these ions. Divalent cations thus have three roles here: they are a factor in the permeability of* C, *in the permeability of* S, *and in the mechanical stability of* A. The latter two roles may, of course, be interdependent.

It is tempting now to venture a few guesses as to the structural equivalents of the elements of the proposed junctional picture. An obvious candidate for the location of the junctional units is the "septate junction," at which the apposing membrane surfaces are periodically cross-linked and which in the present cell system occupies most, if not all, of the cell surfaces of contact (Bullivant and Loewenstein;[4] see also Wood, 1959; Wiener et al., 1964; Locke, 1965; Peachey, 1965, for similar structures; and Robertson, 1963; Farquhar and Palade, 1963; Dewey and Barr, 1964; Pappas and Bennett, 1966, for related structures). The proposed junctional units (many parallel units make up a junction) with all their elements, including the *A* elements, possibly represent the cross-linking "septa" or subunits thereof (see Loewenstein and Kanno, 1964, for a detailed discussion). There are also occasional desmosomes, apparently of the disk-shaped sort, at the contact surfaces. These are, however, unlikely to be involved in electrical coupling, since similar elements are seen between neuroglia and nerve cells which are not electrically coupled (Kuffler and Potter, 1964). These elements are more likely to be concerned with mechanical coupling, as has long been the prevailing idea (for reviews see Studnicka, 1927; Porter, 1956; Fawcett, 1958); and there may well be more than one type of structural element involved in mechanical coupling between cells. Over-all mechanical coupling, in any event, has clearly greater safety margins in respect to all uncoupling agents used than has electrical coupling; the cells do not come apart upon electrical uncoupling.

Some Functional Implications of Uncoupling

UNCOUPLING IN CELL INJURY The phenomenon of membrane sealing by divalent cations is likely to be of physiological significance in cases of cell injury. The capacity of connected cell ensembles for sealing their interiors off from a damaged cell member would seem to offer a means of protection in injury. Indeed, it plays an important role in epithelia exposed to frequent

injury (Loewenstein and Penn, 1967). The elements required for such a sealing reaction are built into the normal system and are critically poised: The Ca^{++} (and Mg^{++} ?) concentration profile falls off steeply across the cell

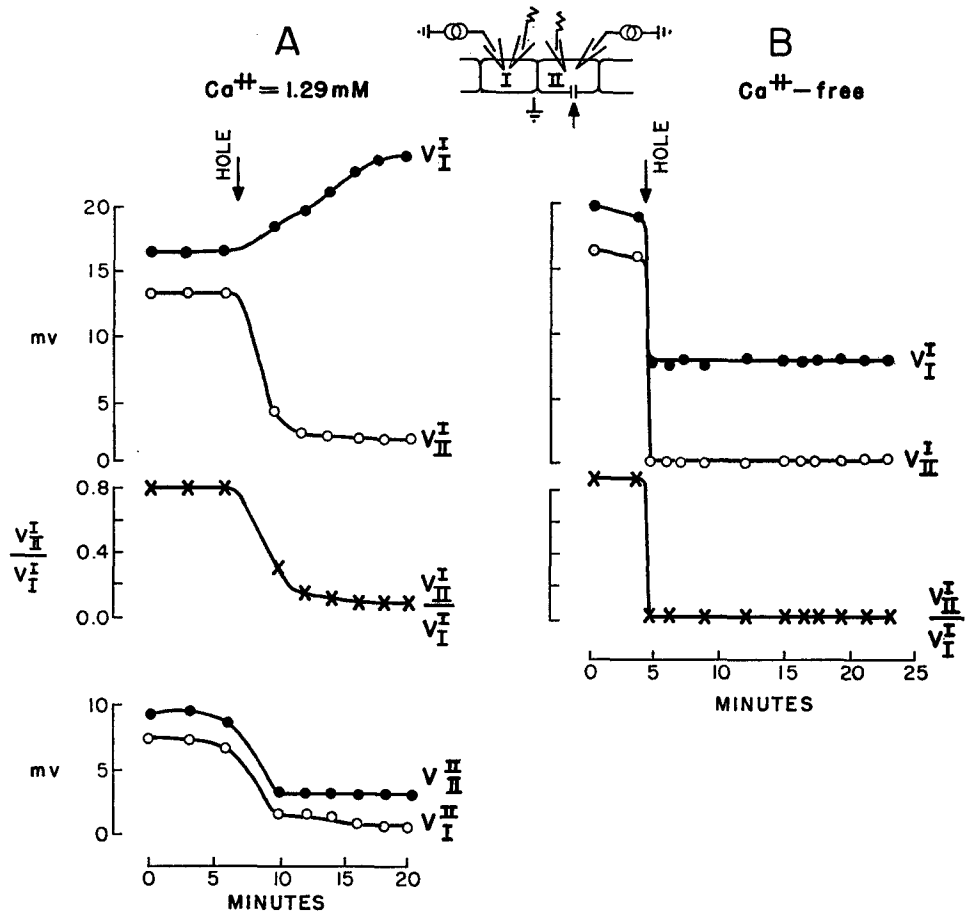

FIGURE 13. Junctional membrane sealing upon cell injury. Current is passed alternately from electrodes in cells *I* and *II*, and the resulting membrane voltages recorded in the two cells (4-electrode arrangement; see inset). The superscript on the membrane voltage denotes the corresponding current-passing electrode. At arrow, hole of a few μ is made in the cell membrane of *II*. A, results obtained in a cell system bathed in normal saline (containing 1.29 mM Ca^{++}); B, in a cell system bathed in Ca^{++}-free saline.

membrane in the inward direction, and the junctional membranes are, evidently, capable of sealing when exposed to sufficiently high [Ca^{++}] or [Mg^{++}]. All that is required to set the reaction in motion is a discontinuity in the cell surface membrane.

This is shown most directly by the experiments illustrated in Figs. 13 and 14,

in which the surface membrane barrier is broken (at *O*). In the experiment of Fig. 13, a hole of a few μ is bored in cell *II* of a cell chain so as to put the junctional membranes of this and the adjacent cell *I* in communication with the extracellular fluid. This causes V_{II} to fall, and V_I to rise when there is 10^{-3} M Ca^{++} in the bathing liquid (A) but not when the $[Ca^{++}]$ is below 10^{-4} M (B). In another type of experiment, relatively large cuts were made into two cells of a chain (Fig. 14). In Ca^{++} concentrations below 10^{-4} M, the system was relatively leaky. In higher Ca^{++} concentrations, V_I rose. In both types of experiments, the rise in V_I was due to sealing of the junctional membranes: the perforated cells stay leaky (Fig. 13 A, V_{II}^{II}), and the effects of the external Ca^{++} on surface membrane resistance are negligible (Fig. 4).

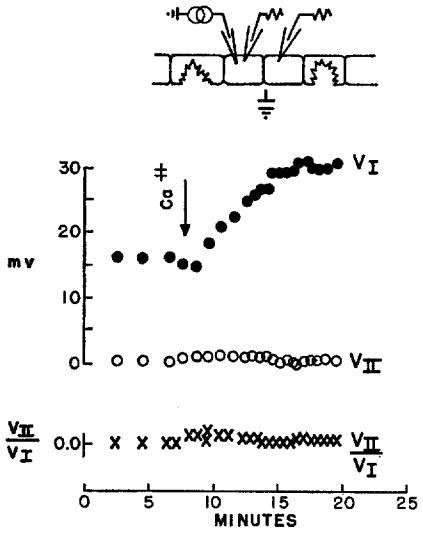

FIGURE 14. Junctional membrane sealing upon cell injury. The cells adjacent to cells *I* and *II* are cut in Ca^{++}-free saline. At arrow, Ca^{++}-free saline is replaced by one containing 2.5 mM Ca^{++}. Recording of V_I and V_{II} starts about 5 min after making of cuts (current 1×10^{-7} amp).

A point of interest brought out by the example in Fig. 14 is that Ca ions can evidently flow through one junction in sufficient quantity to seal a subsequent junction (in this case, between *I* and *II*) before they seal the first.

A sealing mechanism based on Ca^{++} or Mg^{++} may also be at the root of a number of observations of "healing" of injured heart muscle, some dating back to the last century (Engelmann, 1877; Rothschuh, 1951; Weidmann, 1952). These healing phenomena may well be the result of junctional membrane sealing. It is particularly suggestive that the cardiac healing requires Ca^{++} (Délèze, 1965).

PATHOLOGICAL UNCOUPLING The high safety margins make it unlikely that uncoupling occurs in the normal intact cell system. But in pathological situations, local conditions in tissues may conceivably deviate sufficiently to cause uncoupling, or genetic alterations may give rise to uncoupling. A case

in point is liver cancer, where cellular communication is interrupted and where cells behave much like the uncoupled cells here as far as their conductive cell membrane properties are concerned (Loewenstein and Kanno, 1966).

APPENDIX

The cell junction (junction of r_c and r_s, Fig. 3) is not directly accessible to electrical probes. Hence, no measurements can fully define the three resistances r_c, r_s, and r_o. But the related parameters r_j and r of the reduced equivalent circuit (Fig. 15 D) can be determined. From the present results, only lower and upper limits can be set for r_j and r, at least in the normally coupled system. These limits fix useful bounds for r_c; and r provides a lower limit for r_o and, in the normally coupled state, for r_s.

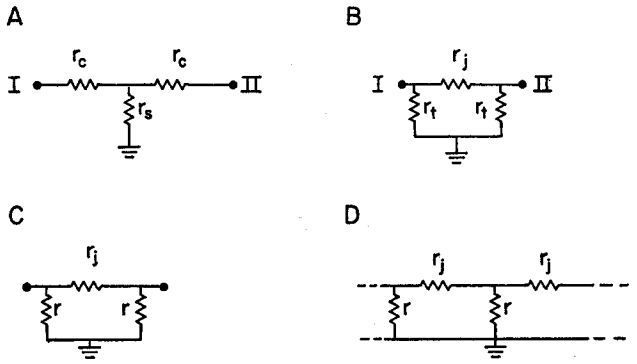

FIGURE 15. Reduced equivalent circuit for the connected cell system. A, a partial repeating element abstracted from equivalent circuit of Fig. 3. B, an equivalent of (A) when measurements are made only between *I*, *II*, and ground. Equations (1)–(4), Appendix. C, reduced electrical equivalent of an isolated coupled cell pair. Equation (5). D, representative repeating elements of reduced electrical equivalent of extended cell chain in Fig. 3. Equation (6).

Analysis of the measurements is restricted by the facts that it was technically too difficult to make measurements in corresponding cells in all glands, and that, failing fully to anticipate analytical problems, we recorded neither the electrode locations in the various experiments nor the number of cells in the chain (though this was generally 20 to 30). Lacking an exact model to fit each case in the normally coupled state, we have bracketed all these cases between a pair of limiting models. In the uncoupled state, the greatly increased junctional resistance makes the length constant considerably smaller than the distance between adjacent cell junctions. Hence, so long as microelectrodes are not in terminal cells of the chain—and they were always at least two cells removed from chain termini—electrode location (and cell number) in the uncoupled state are not critical in analyzing the measurements; any of several discrete models suffices for the computation.

Consider that portion of the equivalent circuit of Fig. 3 which is reproduced in Fig. 15 A. This is indistinguishable from a network of the form in Fig. 15 B when

electrical measurements are made only between the two terminals *I* and *II* and ground. If resistances are then calculated on the assumption of each form, the two sets of resistances are related by

$$r_j = r_c\,(2 + r_c/r_s) \tag{1}$$

and

$$r_t = r_s\,(2 + r_c/r_s) \tag{2}$$

Then, as is readily seen, equal currents from, say, *I* to ground in the two networks give rise to the same potentials between *I*, *II*, and ground in the Fig. 15 A network, as in the Fig. 15 B network. Transformations from parameters of Fig. 15 B to those of Fig. 15 A are

$$r_c = \frac{r_j r_t}{r_j + 2r_t} \tag{3}$$

and

$$r_s = \frac{r_t^2}{r_j + 2r_t} \tag{4}$$

Now, if the electrical pathways through the nonjunctional membranes *O* (resistance r_o) are incorporated the equivalent network for the case of a coupled pair of cells is reducible to the form in Fig. 15 C; and the electrical equivalent of Fig. 3 in the case of an extended chain of cells is reduced to a repeating network of the form in Fig. 15 D. Here,

$$r = \frac{r_o r_t}{r_o + r_t} \tag{5}$$

in a two-cell system, or

$$r = \frac{r_o r_t}{2r_o + r_t} \tag{6}$$

within an extended cell chain. (Equation (6) represents simply an r_o element in parallel with two r_t elements.) The parameters r_j and r of the reduced network are the appropriate ones for an initial analysis since they are the only ones fully definable by the electrical measurements. Subsequent attention to the limits imposed by the value of r upon the possible values of r_o and r_t will give further information about r_c.

In the normally coupled cell chain, transmission line theory provides a satisfactory model for the electrical analysis, since the length constant considerably exceeds the single cell length (Loewenstein et al., 1965). It will be assumed that microelectrodes are centrally positioned within their respective cells, that cells and their junctions throughout the chain have uniform size and conductive properties, and that within the interior of the cell chain all electrical resistance resides in the cell junctions. Let *s*

represent the cell length (hence the distance between electrodes *I* and *II*; cf. Fig. 2, top inset); a, the distance along the cell chain from the center of cell *I* to that end of the chain lying in the direction of cell *II*; and i the magnitude of a steady current passed between the interior of cell *I* and the external ground. Then, from transmission line theory,

$$\frac{V_{II}}{V_I} = \frac{\cosh \frac{a - s}{\lambda}}{\cosh \frac{a}{\lambda}}, \tag{7}$$

where

$$\lambda = s \sqrt{\frac{r}{r_j}}$$

is the length constant. If b represents the distance along the chain from the center of cell *I* to the chain end opposite cell *II*, the input resistance V_I/i is given by the relation

$$\sqrt{r r_j} = \frac{V_I}{i}\left(\tanh \frac{a}{\lambda} + \tanh \frac{b}{\lambda}\right).$$

Since the chain length $(a + b)$ in the present preparation is roughly three times as great as the length constant λ (Loewenstein et al., 1965), it follows that, depending on the location of cell *I*, the value of $\sqrt{r r_j}$ lies between V_I/i and $2V_I/i$.

To arrive at bracketing values for the parameters r_j and r, we consider three alternative electrode placements, corresponding to $a = 2s$, $a = 15s$, and $a = 30s$, respectively. It turns out that among these alternatives, the assumption $a = 2s$ gives the lowest estimate of r:

$$\text{minimum } r = \frac{V_I}{i}\left(\frac{\lambda}{s}\right)_{a=2s}.$$

Similarly,

$$\text{maximum } r = \frac{2V_I}{i}\left(\frac{\lambda}{s}\right)_{a=15s},$$

and

$$\text{minimum } r_j = \frac{V_I}{i}\left(\frac{s}{\lambda}\right)_{a=30s}.$$

The estimate of maximum r, however, must be made differently depending on whether V_{II}/V_I is smaller or larger than about 0.85. For the smaller values of coupling ratio,

$$\text{maximum } r_j = \frac{2V_I}{i}\left(\frac{s}{\lambda}\right)_{a=15s},$$

whereas for the larger values of V_{II}/V_I,

$$\text{maximum } r_j = \frac{V_I}{i}\left(\frac{s}{\lambda}\right)_{a=2s}.$$

To arrive at values of s/λ for each of the three assumed a/s ratios, equation (7) is used together with a table of hyperbolic cosine values, and each value of the coupling ratio is matched in turn by $[\cosh (s/\lambda)]/[\cosh (2s/\lambda)]$, $[\cosh (14s/\lambda)]/[\cosh (15s/\lambda)]$, and $\exp (-s/\lambda)$. The third expression here is essentially equal to the cosh ratio for $a = 30s$; also, the second ratio differs from the third by less than 10% unless the coupling ratio exceeds about 0.9.

In the uncoupled state s/λ is no longer small compared to unity, and the cable approximation must be replaced by a discrete resistance chain model in estimating r_j and r. In most cases the ratio r_j/r becomes so large upon experimental uncoupling that the values of r_j and r can be approximated satisfactorily on the assumption that the impaled pair of cells is in the middle of an infinitely extended chain of cells. For such a network, it can be shown with the aid of Kirchhoff's laws that

$$r_j = \frac{V_I}{i}\left(V_I/V_{II} - V_{II}/V_I\right)$$

and

$$r = \frac{V_I}{i}\left(\frac{V_I + V_{II}}{V_I - V_{II}}\right).$$

When V_{II} falls to the order of a millivolt, it is too poorly defined to be useful in following further changes in r_j. Thus, in most of our experiments, data recorded appreciably later than the time peak V_I was reached, turned out to be unsuited for computation. No computation was done in cases like that of Fig. 2 B, which showed a rapid early fall of V_{II}. In the experiment of Fig. 6, where the coupling ratio had fallen only to 0.38 in the latest useable measurements, the ratio r_j/r was not yet so large as to cut loose the computed estimates from assumptions about electrode location in the cell chain. Thus r_j and r estimates for the "uncoupled" state here were made under special assumptions, except that the network model of the preceding paragraph provided the upper estimate of r. The lower estimate was based on a discrete chain of five cells with cell *I* in the center; the minimum r_j was computed assuming cells *I* and *II*, respectively, to be first and second cells in an infinitely long chain; and maximum r_j, by taking cells *I* and *II*, respectively, as third and second cells in an infinite chain.

To compute lower and upper estimates of r_c in terms of r_j and r, we first eliminate r_t between equations (3) and (6), to obtain

$$\frac{1}{r_c} = \frac{2}{r_j} + \frac{1}{2}\left(\frac{1}{r} - \frac{1}{r_o}\right).$$

If we substitute $r_o = \infty$ (i.e., $r_o \gg r$), the lower limit of r_c may be found. (For the normally coupled state, the lower estimate of r_j and the corresponding value of r,

$$r = \frac{V_I}{i}\left(\frac{\lambda}{s}\right)_{a=30s},$$

are used in evaluating minimum r_c.) The upper limit of r_c follows if $r_o = r$ (i.e., $r_t \gg r_o$) is assumed; then $r_c \approx r_j/2$. (In the computation of maximum r_c for the normally coupled state, maximum r_j is used.) The span between lower and upper r_c limits for the normally coupled state arises mainly from uncertainty about electrode location; in the uncoupled state it reflects the uncertainty about relative sizes of r_o and r_t.

In the normally coupled system, the parameter r is approximately the parallel combination of r_o with r_s, and its value is a lower limit for each of the latter two, the nonjunctional resistances. In the uncoupled system, r may become larger than r_s; but r remains a lower limit for r_o, a limit which r_o approaches more closely the higher r_c rises. In all experiments described, the change in r during uncoupling (i.e., until about the time of peak V_I) was within one order of magnitude at most. In the text, an upper limit of 10 MΩ for r_o in the normally coupled state is estimated on the basis of specific resistances measured in a variety of cell membranes and the area of the outer and luminal membranes of the salivary gland cell. This estimate is comparable to the largest values computed for r in that state (see Table I).

The possibility must be considered that significant rectification occurs at the level of r_o at the large polarization developed during measurements on uncoupled preparations: while this question has not been investigated in the present preparation, rectification under such conditions is common in membranes which, like the *O* element in this case, separate media of widely different ionic composition. But in nearly all experiments in the present work, outward (i.e., depolarizing) currents were used. This means that in all likelihood any rectification would have reduced the resistance r_o in direct relation to the size of current flowing through *O* of a given cell (see e.g., Hodgkin and Katz, 1949). Hence, if such rectification did occur, our computations underestimate the values of r, r_j, and r_c that prevail in the uncoupled state in the absence of large currents. The computations thus still demonstrate clearly that large increases of r_c must occur in such experiments as those of Figs. 2, 5, 6, and 7, and of Table I.

Mr. Ian Baird developed the electrooptically coupled constant-current device (Baird, 1967) and constructed many of the other electronic devices used in the present work. We are indebted to him also for unfailing technical assistance.

We thank also Dr. Asim Jamakosmanovic for assisting with control experiments.

The work was supported by research grants from the National Science Foundation and the National Institutes of Health.

Dr. Nakas is a National Institutes of Health International Fellow in Physiology, from the Institute of Physiology, University of Sarajevo Medical School, Yugoslavia.

Received for publication 23 September 1966.

REFERENCES

BAIRD, I. 1967. A new stimulus isolator for biological application. *Med. Biol. Eng.* **5**: 295.

CHABERECK, S., and A. E. MARTELL. 1959. Organic Sequestering Agents. John Wiley & Sons, Inc., New York.

CHAMBERS, R. 1940. The relation of extraneous coats of organization and permeability of cell membranes. *Cold Spring Harbor Symp. Quant. Biol.* **8**:144.

DÉLÈZE, J. 1965. Calcium ions and the healing-over of heart fibres. *In* Electrophysiology of the Heart. B. Taccardi and G. Machetti, editors. Pergamon Press, Oxford.

DEWEY, M. M., and L. BARR. 1964. A study of the structure and distribution of the nexus. *J. Cell Biol.* **23**:553.

ENGELMANN, T. W. 1877. Vergleichende Untersuchungen zur Lehre von der Muskel- und Nervenelektricität. *Arch. Ges. Physiol.* **15**:116.

FARQUHAR, M. G., and G. E. PALADE. 1963. Junctional complexes in various epithelia. *J. Cell Biol.* **17**:375.

FAWCETT, D. W. 1958. Structural specialization of the cell surface. *In* Frontiers in Cytology. S. L. Palay, editor. Yale University Press, New Haven. 19.

HERBST, C. 1900. Uber das Auseinandergehen von Furchungszellen und Gewebszellen in kalkfreiem Medium. *Arch. Entwicklungsmech. Organ.* **9**:424.

HODGKIN, A. L., and B. KATZ. 1949. The effect of sodium ions on the electrical activity of the giant axon of the squid. *J. Physiol.*, (*London*). **108**:37.

HODGKIN, A. L., and R. KEYNES. 1957. Movements of labelled calcium in squid giant axon. *J. Physiol.*, (*London*). **138**:253.

HOLTFRETER, J. 1948. Significance of the cell membrane in embryonic processes. *Ann. N. Y. Acad. Sci.* **49**:709.

KUFFLER, S. W., and D. D. POTTER. 1964. Glia in the leech central nervous system. Physiological properties and neuron-glia relationships. *J. Neurophysiol.* **27**:290.

LA MER, V. K. 1962. The solubility behavior of hydroxylapatite. *J. Phys. Chem.* **66**:973.

LOCKE, M. 1965. The structure of septate desmosomes. *J. Cell Biol.* **25**:160.

LOEWENSTEIN, W. R. 1966. Permeability of membrane junctions. *Ann. N. Y. Acad. Sci.* **137**:441.

LOEWENSTEIN, W. R. 1967. Genesis of cellular communication. *Develop. Biol.* **15**:503.

LOEWENSTEIN, W. R., and Y. KANNO. 1964. Studies on an epithelial (gland) cell junction. I. Modifications of surface membrane permeability. *J. Cell Biol.* **22**:565.

LOEWENSTEIN, W. R., and Y. KANNO. 1966. Intercellular communication and the control of tissue growth. Lack of communication between cancer cells. *Nature.* **209**:1248.

LOEWENSTEIN, W. R., and R. D. PENN. 1967. Intercellular communication and tissue growth. II. Tissue regeneration. *J. Cell Biol.* **33**:235.

LOEWENSTEIN, W. R., S. J. SOCOLAR, S. HIGASHINO, Y. KANNO, and N. DAVIDSON. 1965. Intercellular communication: renal, urinary bladder, sensory, and salivary gland cells. *Science.* **149**:295.

MOSCONA, A. A. 1952. Cell suspension from organ rudiments of chick embryos. *Exp. Cell Res.* **3**:535.

NAKAS, M., S. HIGASHINO, and W. R. LOEWENSTEIN. 1966. Uncoupling of an epithelial cell membrane junction by calcium-ion removal. *Science.* **151**:89.

PAPPAS, G. D., and M. V. L. BENNETT. 1966. Specialized junctions involved in electrical transmission between neurons. *Ann. N. Y. Acad. Sci.* **137**:495.

PEACHEY, L. 1965. The sarcoplasmic reticulum and transverse tubules of the frog's sartorius. *J. Cell Biol.* **25**:209.

PORTER, K. R. 1956. Observations on the fine structure of animal epidermis. *In Proc. Intern. Conf. Electron Microscopy, 3rd, London, 1954,* 539.

POTTER, D. D., E. J. FURSHPAN, and E. S. LENNOX. 1966. Connections between cells of the developing squid as revealed by electrophysiological methods. *Proc. Natl. Acad. Sci.* **55**:328.

RINALDINI, L. M. J. 1958. The isolation of living cells from animal tissues. *Intern. Rev. Cytol.* **7**:587.

RINGER, S. 1890. Concerning experiments to test the influence of lime sodium and potassium salts on the development of ova and growth of tadpoles. *J. Physiol., (London).* **11**:79.

ROBERTSON, J. D. 1963. The occurrence of a subunit pattern in the unit membranes of club endings in Mauthner cell synapses in goldfish brains. *J. Cell Biol.* **19**:201.

ROTHSCHUH, K. E. 1951. Uber den funktionellen Aufbau des Herzens aus elektrophysiologischen Elementen und über den Mechanismus der Erregegungsleitung im Herzen. *Arch. Ges. Physiol.* **253**:238.

ROUX, P., and F. S. JONES. 1916. A method for obtaining suspensions of living cells from the fixed tissues, and for the plating out of individual cells. *J. Exptl. Med.* **23**:549.

SOCOLAR, S. J., M. NAKAS, and W. R. LOEWENSTEIN. 1967. Junctional uncoupling: labile permeability of a cell membrane junction. *Federation Proc.* **26**:712.

STUDNICKA, F. K. 1927. Die Organisation der lebendigen Masse. *In* Handbuch der mikroskopischen Anatomie des Menschen. W. v. Möllendorff, editor. Springer-Verlag, Berlin. I/1, 421.

WEIDMANN, S. 1952. The electrical constants of Purkinje fibres. *J. Physiol., (London).* **118**:348.

WIENER, J., D. SPIRO, and W. R. LOEWENSTEIN. 1964. Studies on an epithelial (gland) cell junction. II. Surface structure. *J. Cell Biol.* **22**:587.

WOOD, R. L. 1959. Intercellular attachment in the epithelium of Hydra as revealed by electron microscopy. *J. Biophys. and Biochem. Cytol.* **6**:343.